Controls on the variability of net infiltration to desert sandstone

Victor M. Heilweil,[1] Tim S. McKinney,[1] Michael S. Zhdanov,[2] and Dennis E. Watt[3]

Received 19 April 2006; revised 12 March 2007; accepted 13 April 2007; published 18 July 2007.

[1] As populations grow in arid climates and desert bedrock aquifers are increasingly targeted for future development, understanding and quantifying the spatial variability of net infiltration becomes critically important for accurately inventorying water resources and mapping contamination vulnerability. This paper presents a conceptual model of net infiltration to desert sandstone and then develops an empirical equation for its spatial quantification at the watershed scale using linear least squares inversion methods for evaluating controlling parameters (independent variables) based on estimated net infiltration rates (dependent variables). Net infiltration rates used for this regression analysis were calculated from environmental tracers in boreholes and more than 3000 linear meters of vadose zone excavations in an upland basin in southwestern Utah underlain by Navajo sandstone. Soil coarseness, distance to upgradient outcrop, and topographic slope were shown to be the primary physical parameters controlling the spatial variability of net infiltration. Although the method should be transferable to other desert sandstone settings for determining the relative spatial distribution of net infiltration, further study is needed to evaluate the effects of other potential parameters such as slope aspect, outcrop parameters, and climate on absolute net infiltration rates.

Citation: Heilweil, V. M., T. S. McKinney, M. S. Zhdanov, and D. E. Watt (2007), Controls on the variability of net infiltration to desert sandstone, *Water Resour. Res.*, *43*, W07431, doi:10.1029/2006WR005113.

1. Introduction

[2] Net infiltration describes subsurface moisture penetration beneath the root zone, below which water removal by evapotranspiration becomes insignificant [*Scanlon et al.*, 2002; *Flint et al.*, 2002]. Few methods are currently available for examining the spatial distribution of net infiltration and recharge in arid permeable bedrock settings at the watershed scale. This, in part, is a result of complexities associated with the large spatial variability that typically occurs in areas of exposed or shallowly buried bedrock. In addition, rapid urban growth into desert settings with exposed permeable bedrock necessitates the development of accurate aquifer susceptibility maps for avoiding groundwater contamination in high recharge areas. The objective of this study therefore was to develop a conceptual model for describing net infiltration to desert sandstone and a methodology for quantifying desert sandstone net infiltration at the watershed scale, including the ability to accurately differentiate between zones of low and high net infiltration.

[3] The spatial distribution of environmental tracers within the vadose zone, particularly of naturally occurring chloride (Cl) and anthropogenic tritium (^{3}H), often has been used in arid settings to evaluate net infiltration and recharge [*Allison et al.*, 1985, 1994; *Allison and Hughes*, 1974, 1978; *Anderson and Sevel*, 1974; *Edmunds et al.*, 2002; *Izbicki et al.*, 1998; *Phillips et al.*, 1988; *Cook et al.*, 1989, 1992; *Scanlon*, 1991; *Sukhija and Shah*, 1976; *Vogel et al.*, 1974]. Data describing the distribution of these tracers in the subsurface are typically limited to samples from vertical boreholes. These profiles generally show low Cl concentrations and relatively deep penetration of anthropogenic ^{3}H concentrations in areas of focused infiltration, such as beneath washes where active recharge occurs; conversely, high Cl concentrations and relatively shallow penetration of anthropogenic ^{3}H concentrations typically are present in areas of low recharge away from washes. Solutes accumulate in areas of low recharge because evaporation and plant transpiration recycle nearly all soil moisture back to the atmosphere, concentrating the salts from atmospheric deposition (precipitation and dust transport). Boreholes in these areas of high solute accumulation generally have a Cl bulge within 20 m of land surface, generally interpreted as a switch to lower net infiltration rates during the Holocene [*Sharma and Hughes*, 1985; *Cook et al.*, 1989; *Allison et al.*, 1985; *Prudic*, 1994; *Scanlon*, 1991; *Izbicki et al.*, 2002]. Because of the expense and time involved with borehole drilling and core collection, however, few detailed studies have been conducted to investigate the spatial distribution of environmental tracers for assessing the degree of variation in net infiltration at the basin scale, particularly in bedrock settings.

[4] Several studies have used least squares regression analyses [*Cherkauer and Ansari*, 2005; *Lorenz and Delin*, 2005] and GIS-based methods [*Braun et al.*, 2003; *Flint et al.*, 2004; *Kwicklis et al.*, 2005] for evaluating parameters controlling spatial variability and developing empirical and/or water budget methods for estimating net infiltration and groundwater recharge. Typical controlling parameters

[1] U.S. Geological Survey, Salt Lake City, Utah, USA.
[2] Department of Geology and Geophysics, University of Utah, Salt Lake City, Utah, USA.
[3] U.S. Bureau of Reclamation, Boulder City, Nevada, USA.

0043-1397/07/2006WR005113$09.00

reported are soil properties, topography (steepness and aspect), precipitation, and vegetation/evapotranspiration [*Charles et al.*, 1993; *Delin et al.*, 2000; *Holtschlag*, 1997; *Kwicklis et al.*, 2005], but also include air temperature, bedrock permeability, land use, porosity, and depth to water table [*Arnold and Friedel*, 2000; *Cherkauer*, 2004; *Flint et al.*, 2004].

[5] Recent studies of outcropping and soil-covered Navajo sandstone in the upper Mojave Desert have shown large spatial variability in both (1) vadose zone solute distributions in sandstone excavations [*Heilweil and Solomon*, 2004], and (2) net infiltration rates based on environmental tracer profiles from boreholes [*Heilweil et al.*, 2006]. Net infiltration rates ranged over two orders of magnitude, determined using both the Cl mass balance method and the ^{3}H depth-to-peak and mass balance methods in a variety of topographic and morphologic settings. In this paper, we (1) develop a conceptual model of net infiltration to desert sandstone based on observed spatial variability, (2) use numerical inversion (least squares regression) techniques to determine the important physical parameters controlling net infiltration, and (3) apply GIS methods to this empirical model to predict basin-scale net infiltration rates.

2. Concepts of Net Infiltration and Recharge to Desert Sandstone

[6] For this paper, net infiltration is defined as the percolation flux that passes beneath the depth of the root zone [*Scanlon et al.*, 2002; *Flint et al.*, 2002]; therefore ''net infiltration depth'' is considered synonymous with the maximum depth of the root zone. ''Groundwater recharge,'' herein referred to as ''recharge,'' is defined as water entering the aquifer at the water table. Net infiltration and recharge rates may be equivalent if conditions remain uniform while water is moving through the vadose zone to the water table, unless diverted laterally to a perched seep or spring [*de Vries and Simmers*, 2002; *Freeze and Cherry*, 1979; *Flint et al.*, 2001a, 2001b].

[7] The conceptual model of net infiltration and recharge to desert sandstone (Figure 1) includes two main processes: (1) direct infiltration and percolation of precipitation through both outcropping and soil-covered sandstone, and (2) focused infiltration and percolation through exposed sandstone fractures or soils receiving runoff directly downgradient of outcrop areas [*Cordova et al.*, 1972; *Cordova*, 1978; *Hood and Danielson*, 1981; *Eychaner*, 1983; *Hood and Patterson*, 1984]. ''Direct infiltration'' is water entering the subsurface from on-site precipitation, whereas ''focused infiltration and percolation'' is water that is focused either above land surface (along washes or channels) or at the soil/bedrock contact prior to penetrating the bedrock.

2.1. Direct Infiltration

[8] The amount of direct infiltration through exposed (nonvegetated) permeable bedrock is dependent upon many factors such as permeability, topographic slope and aspect, fracture density, bare-surface evaporation (function of solar radiation, temperature, relative humidity, wind speed), and precipitation [*Flint et al.*, 2001a]. A study by *Rasmussen and Evans* [1993] determined relatively high infiltration rates on exposed permeable bedrock, with surface fractures playing a critical role in the infiltration process. One might speculate that there also would be a correlation between recharge and fracture orientation, with higher recharge rates expected when fractures are perpendicular to topographic slope.

[9] In addition to these parameters, the amount of direct infiltration at soil-covered locations is controlled by evapotranspiration and soil hydraulic properties [*Olofsson*, 1994; *Stothoff et al.*, 1999; *Stephens*, 1996]. Thin coarse-grained soils with low antecedent moisture will allow for more rapid gravity drainage and net percolation to underlying bedrock (minimizing bare soil evaporation and plant transpiration) than thick fine-grained soils with higher water storage capacity [*Wilson and Guan*, 2004; *Flint et al.*, 2004; *Tindall and Kunkel*, 1999; *Buttle and McDonald*, 2002].

2.2. Focused Infiltration

[10] Focused infiltration to desert sandstone is primarily caused by runoff during high-intensity precipitation events from sloping sandstone outcrops. Focusing likely first occurs at open fractures along the outcrop (Figure 1). Exposed bedrock fractures increase net infiltration because of their ability to divert runoff and readily transmit this water to the subsurface [*Rasmussen and Evans*, 1993]. The shallow parts of near-vertical sandstone fractures are typically open or sand filled in areas of outcropping sandstone, yet have a calcrete and root fill where the sandstone is soil covered. Detailed shallow vadose zone solute patterns in and around near-vertical sandstone fractures indicate that open fractures act as conduits for infiltration, whereas calcrete and root-filled fractures inhibit infiltration because of a combination of the lower-permeability fracture fill and plant transpiration [*Heilweil and Solomon*, 2004]. The enhanced effects of fracturing on net infiltration therefore likely are primarily along areas of exposed sandstone. Because of attenuation caused by matrix imbibition into surrounding unsaturated porous bedrock [*Nitao and Busheck*, 1991], these preferential flow effects likely are smoothed in the deeper vadose zone.

[11] Focusing also occurs immediately downgradient of bedrock outcrop areas through soils that can temporarily retain runoff from the outcrop [*Flint et al.*, 2001c]. Water readily infiltrates at these locations because the soils here are derived from the weathered bedrock outcrop and are generally coarser and more permeable than soils lower in a basin. Depending on the permeability reduction at the soil/bedrock interface, this water either becomes perched or infiltrates into the underlying media [*Stephens*, 1996]. Such ponding has been observed at the soil/bedrock interface in the Sierra Mountains [*Flint and Flint*, 2006]. In desert settings, the contrast is enhanced by the development of low-permeability calcrete deposits, which can have saturated hydraulic conductivity values as low as two orders of magnitude less than that of sandstone [*Heilweil and Solomon*, 2004]. Calcrete in the Mohave and other deserts is formed by solute concentration and carbonate supersaturation/precipitation from evapotranspiration [*Cerling*, 1984; *Quade et al.*, 1989; *Schlesinger*, 1985]. Ponded water not used by these plants either slowly infiltrates the sandstone or continues along the sloping bedrock contact, where it either is subsequently intercepted by plant roots and transpired back to the atmosphere or infiltrates the sandstone. The amount of this ''focused'' infiltration and percolation therefore decreases away from the outcrop runoff source.

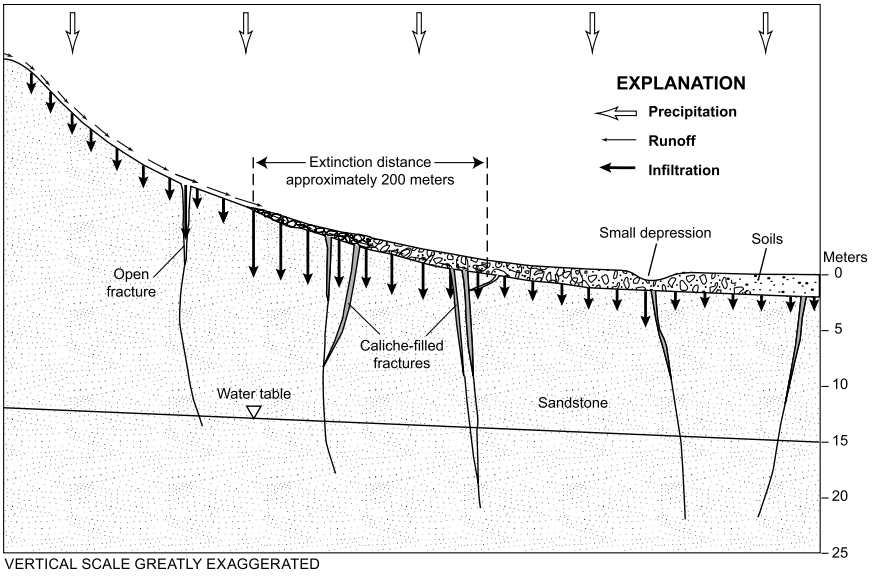

Figure 1. Conceptual model of net infiltration to fractured sandstone.

Microtopography (small depressions) and heterogeneity of calcrete also may cause variability in this focused infiltration and percolation [*Derby and Knighton*, 2001; *Klock*, 2003]. The maximum distance of this downgradient movement will depend on the amount of runoff and infiltration reaching the sandstone contact (a function of outcrop area, permeability, slope and aspect, soil properties, and precipitation intensity) and seasonally dependent plant transpiration. It is hypothesized that larger, nonfractured, steeper, north facing outcrop areas would likely produce more runoff and therefore higher net infiltration rates in downgradient soil-covered sandstone than smaller, fractured, gently sloping, south facing outcrops.

2.3. Vegetation and Soils

[12] Vegetation type and density (and resultant transpiration) are closely related to soil properties. Finer-grained and thicker soils will have a larger water storage capacity, impeding gravity drainage to underlying sandstone and increasing water available for plant consumption [*Flint et al.*, 2001c]. Also, it is speculated that more moisture will be available for plant use in areas receiving runoff from upgradient outcrop areas. Previous plant survey studies of soil-covered desert bedrock have shown that plant density is correlated to water storage capacity, a function of soil grain size distribution and thickness [*Stothoff et al.*, 1999].

[13] In summary, net infiltration and recharge to desert sandstone can be described by a combination of the following possible physical parameters: climate (precipitation, temperature, solar radiation, wind speed, and relative humidity); soils (coarseness, thickness, distance from exposed outcrop, antecedent moisture); topography (slope, aspect); exposed outcrop (size, slope, aspect, fracture density); and buried sandstone fracture density (Table 1).

3. Site Description

[14] The Navajo sandstone is a fine-grained, well-sorted eolian sandstone of the Colorado Plateau Glen Canyon Formation, which covers a large part of the southwestern United States [*Robson and Banta*, 1995]. Because of its relatively high permeability and thickness (as much as 600 m), it forms a major regional aquifer [*Cordova et al.*, 1972; *Hurlow*, 1998]. Detailed field studies at Sand Hollow, an upland basin (880–1260 m altitude) of the Mojave Desert ecosystem 15 km northeast of St. George, Utah (Figure 2), provide a means for testing pieces of the above conceptual model of net infiltration to desert sandstone. The Navajo sandstone at Sand Hollow is either exposed or covered with thin soils (Figure 3). Its hydraulic properties are relatively homogenous. Laboratory analysis of 17 samples had ranges in porosity and saturated hydraulic conductivity of 0.20–0.27 and 0.01–0.42 m/d, respectively. Prior to the construction of an off-stream surface water reservoir, the underlying sandstone aquifer was unconfined, with depths to groundwater in the lower basin ranging from 15 to 65 m [*Heilweil et al.*, 2005]. During reservoir construction, three excavations were cut into the shallow vadose zone: Trench 1 (1000 m) oriented along a strike of 115° in the lower basin; Trench 2 (1900 m) oriented along a strike of 35° on the

Table 1. Potential Parameters Controlling Net Infiltration to Desert Sandstone

Category	Parameter	Evaluated in This Study?
Climate	precipitation	yes
Climate	temperature	no
Climate	solar radiation	no
Climate	wind speed	no
Climate	relative humidity	no
Soils	coarseness	yes
Soils	thickness	yes
Soils	distance from exposed outcrop	yes
Soils	antecedent moisture	no
Topography	slope	yes
Topography	aspect	no
Exposed outcrop	size	no
Exposed outcrop	slope	no
Exposed outcrop	aspect	no
Exposed outcrop	fracture density	no
Buried sandstone	fracture density	yes

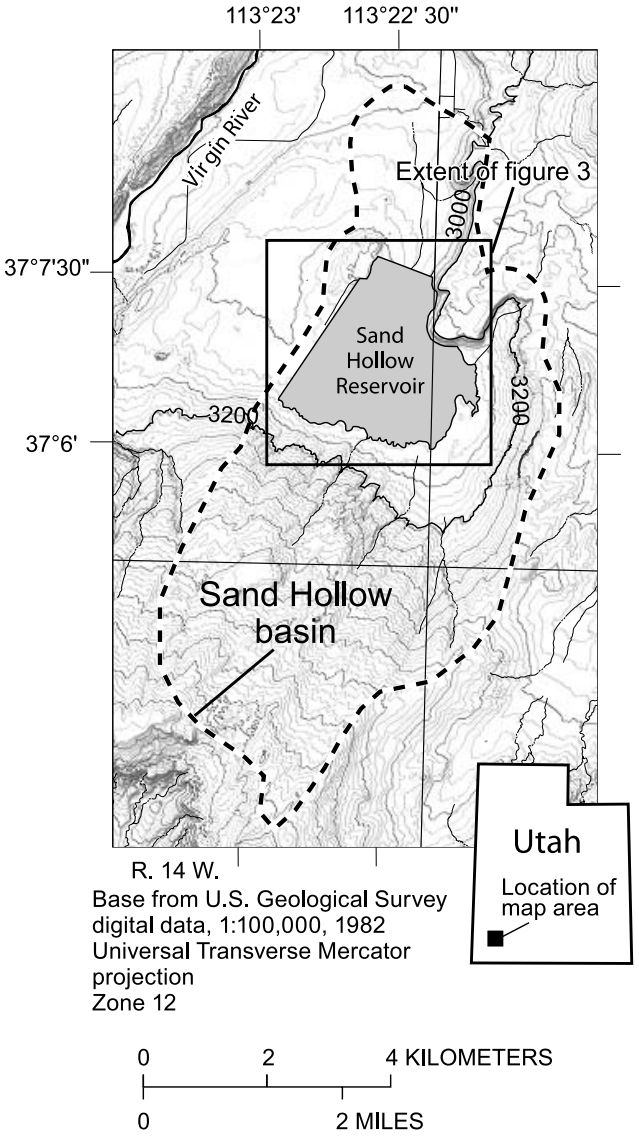

Figure 2. Location of Sand Hollow, southwestern Utah.

western side of the watershed, and the East Ridge road cut (450 m) oriented along a strike of 60° beneath the East Ridge (Figure 3). Near-vertical (55° to 90° dip) fractures with an average but nonuniform spacing of about 5 m and strike of 40° were observed in the sandstone excavations [*Heilweil and Solomon*, 2004]. The fractures are typically continuous vertically and open along the exposed outcrop, yet filled with calcrete to a depth of about 3 m beneath soil-covered areas. Fracture aperture is generally less than 20 mm and decreases with depth. Roots and caliche were observed in unconsolidated soils and shallow parts of fractures, but not in nonfractured sandstone, nor deeper than about 3 m in fractures.

4. Methods

[15] All of the potential parameters controlling net infiltration to desert sandstone, including the six field parameters that were evaluated during this study, are listed in Table 1. Plant evapotranspiration and bare-surface evaporation were not considered to be independent parameters because of the correlation between soil properties and plant density. Similarly, bare-surface evaporation is a climate variable that is dependent on temperature, wind speed, relative humidity, precipitation, and solar radiation (a function of elevation, latitude, topographic slope, and aspect). Because temperature, wind speed, relative humidity, and solar radiation are assumed to be relatively constant in Sand Hollow (no south facing slopes), variation in bare-surface evaporation is assumed to be controlled primarily by topographic slope and precipitation. Other potential parameters that were not evaluated during this study include antecedent soil moisture and exposed outcrop parameters (size, slope, aspect, fracture density). Antecedent soil moisture is a function of soil coarseness and thickness, and thus not considered an independent parameter. There was insufficient trench and borehole solute data at Sand Hollow for a meaningful evaluation of net infiltration caused by variation in exposed outcrop parameters.

4.1. Field Parameter Measurements

[16] Field values for five of the potential parameters controlling net infiltration (soil thickness, soil coarseness, distance from exposed outcrop, topographic slope, and buried sandstone fracture density) were collected shortly after the excavations in Sand Hollow were completed. Soil thickness and soil coarseness data were collected at a 30-m offset because of soil disturbance along the excavations. Soil thickness was determined by hand auguring to the sandstone contact. Soil coarseness of material finer than 19 mm was determined by sieve analysis [*U.S. Bureau of Reclamation*, 1990a, 1990b] and presented as the fraction of soil coarser than 0.15 mm. Soil coarseness varied by less than 25% along vertical profiles at three sites shown in Figure 3. The West Dam site (interval number 3) had an arithmetic mean soil coarseness fraction of 61 ± 5.6 (1σ) for six sample depths; the North Dam site (interval number 34) had an arithmetic mean soil coarseness fraction of 43 ± 4 (1σ) for five sample depths; and Borehole site number 2 had an arithmetic mean soil coarseness fraction of 64 ± 5.4 (1σ) for four sample depths. This indicates that surficial soil coarseness is representative of the entire soil column to the bedrock contact. Fracture density was determined by mapping fracture traces, using the intersection of nonbedding plane high-angle (55° to 85° dip) fractures with 1-m horizontally spaced grid lines demarcated along the walls of the excavations (Alpha Engineering, written communication, 2000). Downgradient distance from sandstone outcrop was determined by survey markers or measuring tape along the steepest descent direction (downgradient path of surface water runoff): intervals 13 through 48 along Trench 1 use distance to exposed sandstone of the West Ridge; intervals 49 through 68 and all intervals (69–94) of the East Ridge road cut use distance to the East Ridge basalt outcrop. For Trench 2 (intervals 1–12), the distance was set to 30 m, based on proximity to numerous small sandstone outcrops. Topographic slopes were calculated from total station GPS altitude surveying at a 15-m horizontal spacing density (with submeter vertical accuracy) prior to soil removal (Alpha Engineering, written communication, 2000).

[17] Precipitation, another field parameter, was determined from 30-year (1971–2000) average annual Natural Resour-

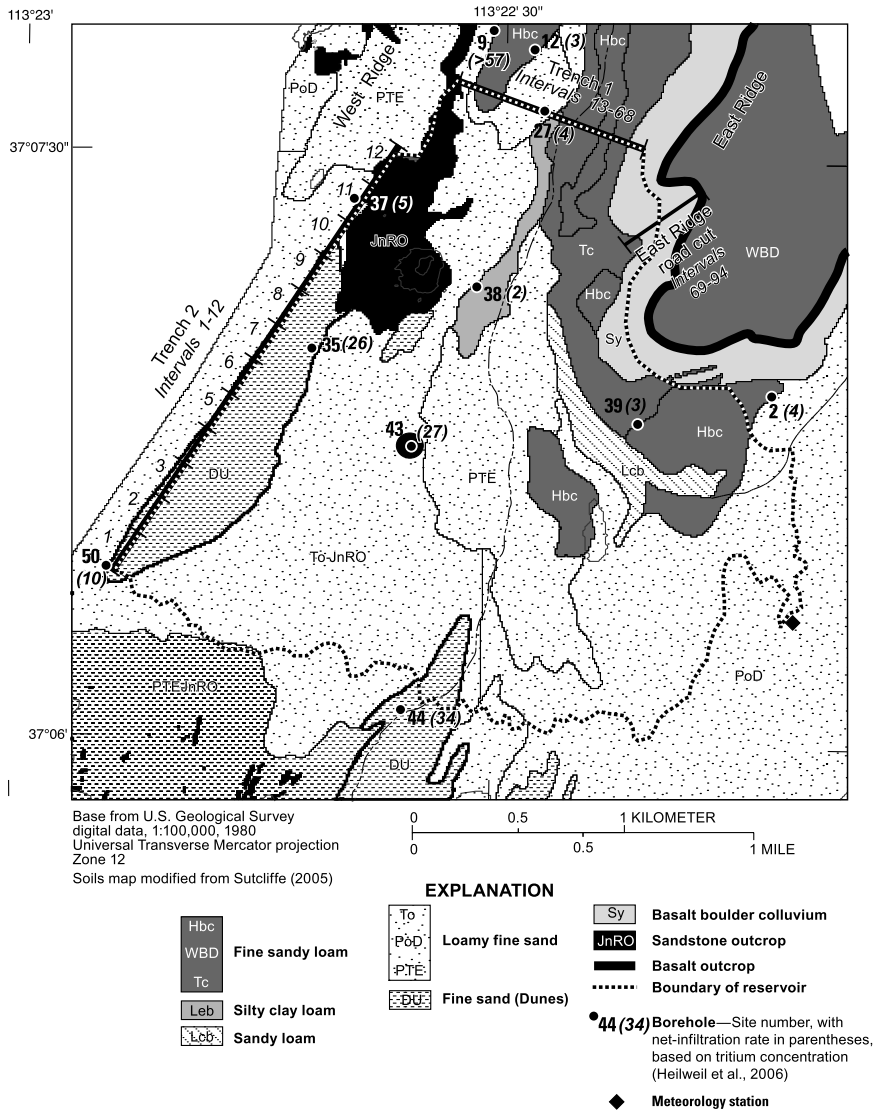

Figure 3. Soils map with location of excavation intervals and boreholes in Sand Hollow, Utah.

ces Conservation Service (NRCS) Parameter-elevation Regressions on Independent Slopes Model (PRISM) data (Spatial Climate Analysis Service, Oregon State University, created 4 April 2004 and accessed in April 2005 at http://www.ocs.oregonstate.edu/prism/). Because of its large grid size (4-km^2 cells), the original precipitation grid was resampled to 0.25-km^2 grid cells [*McCoy et al.*, 2001], resulting in values of 200 to 250 mm/yr in Sand Hollow. Data for 1998–2004 from the meteorology station (Figure 3) closely correlates with historical (1893–2004) precipitation data from nearby St. George, Utah (Western Regional Climate Center, Monthly and annual precipitation at St. George, Utah (station 427516), accessed 11 February 2004 at http://www.wrcc.dri.edu/) and indicates a long-term average rate of 220 mm/yr, same as the resampled average PRISM value for this site.

4.2. Net Infiltration Estimates Along Excavations

[18] Net infiltration estimates are based on vadose zone specific conductance (Sc) values of leachates collected along the entire 3350 m of excavations [*Heilweil and Solomon*, 2004] and environmental tracers (^{3}H, Cl) in 11 boreholes [*Heilweil et al.*, 2006] (Figure 4). Each of the excavations in Sand Hollow was divided into intervals according to sampling frequency, solute accumulation, and soil cover, resulting in a total of 94 intervals for the estimation of net infiltration rates. Because variable numbers of samples for leachate analysis were collected, geometric mean values were calculated for each interval. A subset of leachate samples previously analyzed for both Sc and Cl resulted in a Cl/Sc ratio of 0.27 ($n = 76$, $r^2 = 0.99$) [*Heilweil and Solomon*, 2004]. The borehole Cl profiles show maximum chloride values at an average depth of about 5 m (Table 2), the same approximate depth as leachate sample collection in the excavations. It is assumed therefore that the Sc values of the excavations represent peak concentrations of solute accumulation. Net infiltration rates determined previously by using the vadose zone ^{3}H depth-to-peak method [*Cook et al.*, 1994] ranged from 2 to more than 57 mm/yr at 11 borehole locations in Sand Hollow [*Heilweil et al.*, 2006] (Figure 3). Dividing the recharge rate at each

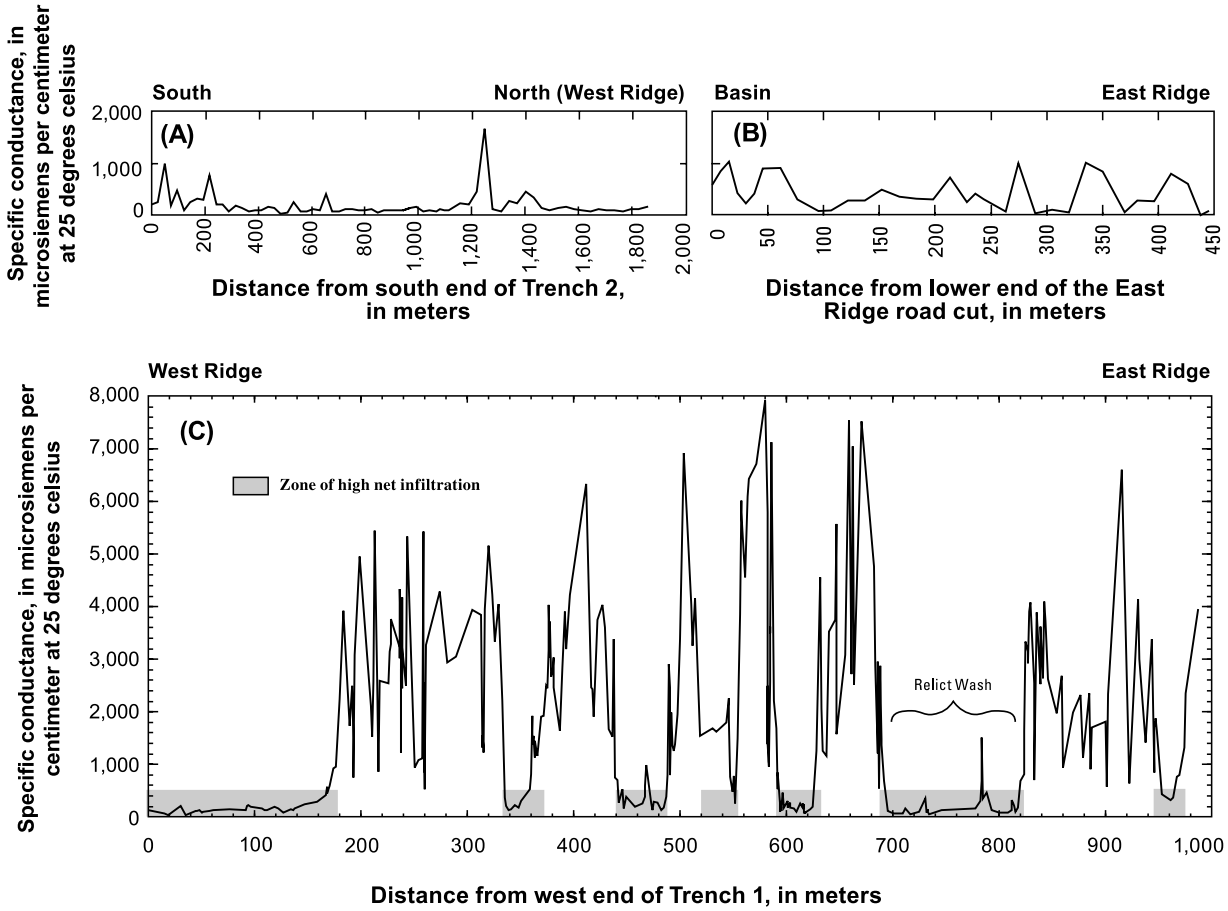

Figure 4. Specific-conductance values of leachates from sandstone samples at a depth of about 5 m along (a) Trench 2, (b) East Ridge road cut, and (c) Trench 1, in Sand Hollow, Utah [from *Heilweil and Solomon*, 2004].

location by the precipitation rate yields the average annual net infiltration ratio. These average annual net infiltration ratios (R) range from 0.01 to 0.28 for the 11 borehole locations (Table 2). There is a strong correlation ($r^2 = 0.85$; Figure 5) between these net infiltration ratios and the peak vadose zone Cl concentration from each borehole:

$$R = 0.88(\mathrm{Cl})^{-0.5}. \quad (1)$$

[19] On the basis of the Cl:Sc ratio given above of 0.27, this yields the relation

$$R = 1.7(Sc)^{-0.5}. \quad (2)$$

[20] Equation (2) is then used with mean Sc value for each of the 94 excavation intervals for estimating net infiltration ratios. Although the theoretical form of the relation between chloride concentration/specific conductance and recharge rate based on the CMB method is linear, data from Sand Hollow show an interesting nonlinear relation, justifying the use of the empirical inverse square root relation (Figure 5).

4.3. Inverse Methods

[21] Linear least squares inversion methods were used to determine an empirical relation between net infiltration

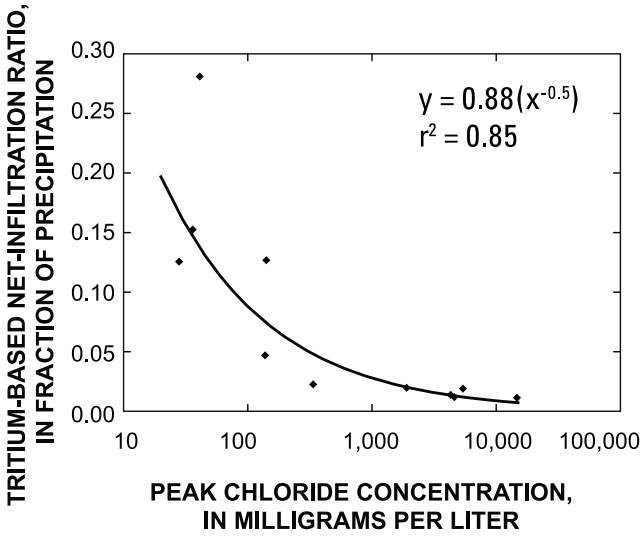

Figure 5. Relation between tritium-based net infiltration ratio and peak chloride concentration for vadose zone boreholes in Sand Hollow, Utah.

Table 2. Peak Pore Water Chloride Concentration and Depth, Tritium-Based Net Infiltration Rate, Precipitation Rate, and Net Infiltration Ratio for Borehole Sites in Sand Hollow, Utah

Site Number[a]	Peak Pore Water Chloride Concentration, mg/L	Depth of Chloride Peak, m	Tritium-Based Net Infiltration Rate,[b] mm/yr	Precipitation Rate, mm/yr	Tritium-Based Net Infiltration Ratio R	GIS-Predicted Net Infiltration Rate, mm/yr
9	40	6	57 ± 7[c]	200	0.28[c]	25
44	40	6	34 ± 5	220	0.15	35
43	140	3	27 ± 4	210	0.13	21
35	30	7	26 ± 3	210	0.13	26
50	140	6	10 ± 2	210	0.05	19
37	340	5	5 ± 2	200	0.02	11
2	5,400	5	4 ± 2	220	0.02	4
27	1,900	6	4 ± 2	200	0.02	20
12	4,300	5	3 ± 1	200	0.01	4
39	4,600	6	3 ± 1	220	0.01	4
38	14,700	2	2 ± 1	210	0.01	4

[a]Site number: refer to Figure 3.
[b]Rate and uncertainty reported by *Heilweil et al.* [2006]; uncertainty calculation based on work by *Ang and Tang* [1975].
[c]Minimum infiltration rate and ratio because tritum peak already passed through the unsaturated zone, on the basis of high water table tritium concentrations.

ratios at Sand Hollow and these five potential controlling parameters. It was not known a priori whether net infiltration ratios are controlled by a linear or nonlinear combination of the potential controlling parameters, so the generic form of the empirical equation includes both quadratic and cubic terms:

$$R_n = m_1A_1 + m_2A_2 + m_3A_3 + m_4A_4 + m_5A_5 + m_6A_6 + m_7A_7 + m_8A_8 + m_9A_9, + m_{10}A_{10} + m_{11}A_{11} + m_{12}A_{12} + m_{13}A_{13} + m_{14}A_{14} + m_{15}A_{15}, \quad (3)$$

where R_n is the vector of estimated net infiltration ratios, $m_{1\text{-}15}$ are weighting functions, A_1 is soil thickness in m, A_2 is grain size in percent coarser than 0.15 mm, A_3 is sandstone fracture density in number of fractures per linear meter, A_4 is downgradient distance from sandstone outcrop in m, A_5 is topographic slope in percent, A_6 through A_{10} are $(A_1)^2$ through $(A_5)^2$, and A_{11} through A_{15} are $(A_1)^3$ through $(A_5)^3$. Because the number of estimated net infiltration ratios, R (94), are greater than the maximum number of weighting functions, m (15), the system is over determined and A is a rectangular matrix. Therefore rather than solving for an exact set of values, an optimized set of coefficients (m) yielding the smallest misfit between estimated (R) and predicted (R^p) net infiltration ratios were calculated [*Zhdanov*, 2002].

4.4. Borehole ^{3}H Measurements

[22] To evaluate the accuracy of using surface parameters for predicting net infiltration rates to desert sandstone outside of the study area, an additional vadose zone borehole was drilled for determining ^{3}H-based net infiltration rates at Anderson Junction, about 15 km north of the study area. Pore waters were extracted from core samples by cryodistillation and analyzed for ^{3}H at the University of Utah Dissolved Gas Service Center on a mass spectrometer with the helium in-growth method [*Clark et al.*, 1976]. Portions of the core samples also were weighed and then oven dried at 105°C for 24 hours to determine gravimetric water content. Gravimetric water content was converted to volumetric water content by using a bulk density representative of the Navajo sandstone at Sand Hollow of 1,980 ± 110 kg/m^3 [*Heilweil et al.*, 2006].

5. Results

5.1. Net Infiltration Estimates

[23] The calculated geometric mean Sc value for each of the 94 excavation intervals in Sand Hollow ranged from 48 to 3940 μS/cm. These values are used in equation (2) to calculate estimated net infiltration ratios ranging from 2.7% to 24.6% of average annual precipitation (online Table S1[1]) and used as observed data, R_n, in equation (3) for application of the linear inversion methods. On the basis of the estimated annual precipitation of about 200 mm/yr along the excavations, estimated net infiltration rates range from about 5 to 50 mm/yr. Because of the similar topography and soil cover (basalt boulder colluvium) at the east end of Trench 1 and along the lower end of the East Ridge road cut, the Sc profile of the road cut can be considered an approximate extension of Trench 1. Similarly, a continuum is assumed between the two trenches because the north end of Trench 2 and the west end of Trench 1 both intersect exposed sandstone of the West Ridge. Thus the estimated net infiltration rates from the 94 excavation intervals in Sand Hollow are presented as one continuous cross section (Figure 6). All of the Trench 2 intervals (1–12) have high net infiltration rates (>20 mm/yr), likely caused by a combination of coarser soils and runoff from small nearby outcrop areas. Similarly high rates along the west side of Trench 1 (intervals 13–21) are caused by downgradient runoff from a large outcrop area along the West Ridge. On the basis of this zone of high net infiltration rates, a maximum (extinction) distance of 200 m is assumed throughout Sand Hollow for the effects of enhanced infiltration downgradient from outcrop runoff. Except for three other narrow zones, the rest of the Trench 1 intervals (21–68) have generally low infiltration rates of less than 10 mm/yr. Net infiltration rates along the East Ridge road cut (intervals 69–94) are quite variable, particularly intervals 84–91

[1]Auxiliary materials are available at ftp://ftp.agu.org/apend/wr/2006wr005113.

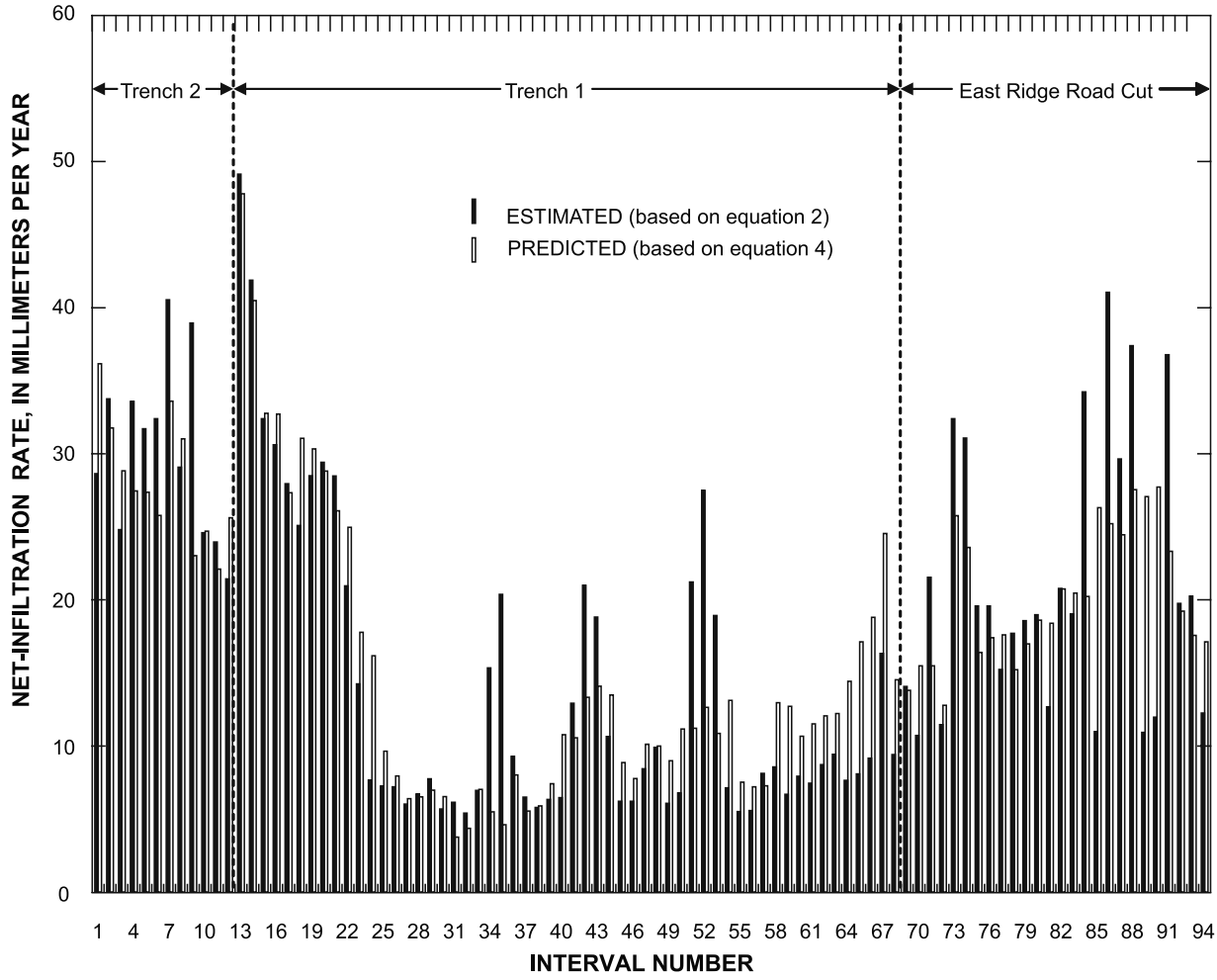

Figure 6. Estimated and model-predicted net infiltration rates using the three surface parameters (soil coarseness, downgradient distance from outcrop, and topographic slope) along excavations in Sand Hollow, Utah.

where large boulders in the colluvium both generate small amounts of runoff for focused infiltration, yet also create a shadow effect by forming an impermeable barrier to direct infiltration.

5.2. Measured Parameter Values and Inversion Results

[24] Measured parameter values were assigned for each interval along the excavations and used for operator matrix A of the linear inversion (online Table S2). Soil thickness (A_1) ranges from 0.0 to 3.35 m. Soil coarseness (A_2), defined as the fraction coarser than 0.15 mm, ranges from 0.18 to 0.86. Fracture density (A_3), reported as the number of high-angle fractures per linear meter of excavation, ranges from 0.0 to 0.86 and averaged 0.19 fractures per meter. The average fracture density for the individual excavations was 0.21, 0.19, and 0.16 fractures per meter, respectively, for Trench 1, Trench 2, and the East Ridge road cut, consistent with the orientation of these excavations with respect to the predominant 40° regional fracture strike in Sand Hollow [*Heilweil and Solomon*, 2004]. Downgradient distance from outcrop (A_4) ranges from 0 to 200 m, the maximum extinction distance discussed earlier. Topographic slope (A_5) ranged from 0.02% to 30%.

[25] Linear least squares inversion methods were applied by using an operator matrix with different combinations of linear, quadratic, and cubic terms to determine empirical relations among these potential controlling parameters (A_1 though A_5) and the estimated net infiltration ratios, (R_1 through R_{94}). The resulting misfit between estimated and predicted net infiltration ratios using all five linear terms (A_1 through A_5) is 35%. The misfit improved to 21% by including quadratic terms for each input parameter. The inclusion of cubic terms did not further reduce the misfit.

[26] Soil thickness and fracture density are subsurface parameters that can be determined only from costly excavations, whereas the other three are surface parameters (A_2, soil coarseness; A_4, downgradient distance from outcrop; and A_5, slope) that can be more easily quantified from topographic and soils maps (aided by laboratory sieve analysis of characteristic soil types). Correlation coefficients (Table 3) indicate that estimated net infiltration rates are less affected by the two subsurface parameters than the three surface parameters. Sensitivity analyses were conducted using linear and quadratic terms of only four parameters at a time (sequentially leaving out each of the five parameters). The results of this exercise were consistent with the correlation coefficients in Table 3, showing that the misfit remained about the same when fracture

Table 3. Correlation Coefficient and Covariance for Five Potential Parameters Controlling Net Infiltration Along the 94 Excavation Intervals in Sand Hollow, Utah

	A_1: Soil Thickness	A_2: Soil Coarseness	A_3: Fracture Density	A_4: Distance From Outcrop	A_5: Topographic Slope
			Correlation Coefficient		
A_1: Soil thickness	1.00	−0.450	0.075	−0.115	0.456
A_2: Soil coarseness		1.00	−0.005	−0.475	−0.555
A_3: Fracture density			1.00	0.173	−0.184
A_4: Distance from outcrop				1.00	−0.188
A_5: Topographic slope					1.00
Estimated net infiltration	0.003	0.124	0.052	0.480	0.077
			Covariance		
A_1: Soil thickness	0.393	−0.055	0.008	−5.47	0.024
A_2: Soil coarseness		0.038	0.000	−7.01	−0.009
A_3: Fracture density			0.028	2.20	−0.003
A_4: Distance from outcrop				5790	−1.20
A_5: Topographic slope					0.007

density and soil thickness were not included. However, eliminating distance to outcrop, soil coarseness, or topographic slope increased the misfits to 26%, 36%, and 39%, respectively. Therefore the linear least squares inversion was recalculated for just these three surface parameters (using both linear and quadratic terms), producing an average misfit of 21%, the same as the model including all five parameters. This confirms that soil thickness and fracture density are not important controlling parameters for net infiltration at Sand Hollow. Reducing equation (3) to a simpler empirical relation using only surface parameters yields

$$R_n = m_2A_2 + m_4A_4 + m_5A_5 + m_7(A_2)^2 + m_9(A_4)^2 + m_{10}(A_5)^2, \quad (4)$$

where m_2 is 1.78×10^{-1} 1/mm, m_4 is 1.74×10^{-4} 1/m, m_5 is 1.07, m_7 is -2.73×10^{-2} 1/mm^2, m_9 is -2.06×10^{-6} 1/m^2, and m_{10} is −3.14. It is noted that equation (4) does not have a constant because zero values for all parameters would result in a net infiltration ratio of zero, as is the case for a soil having a value of zero for coarseness fraction of material coarser than 0.15 mm (a fine-grained soil), a downgradient distance of zero from the nearest upgradient outcrop, and a topographic slope of 0%. Data from Sand Hollow indicate that there is no recharge occurring in areas having a combination of fine-grained soils (no direct infiltration) and no surface runoff (no focused infiltration). This is consistent with studies of other alluvial desert basins receiving similar amounts of precipitation, where little or no basin floor recharge away from washes occurs under present climatic conditions [*Phillips*, 1994; *Tyler et al.*, 1996; *Izbicki et al.*, 2002].

[27] Multiplying R_n by the average annual precipitation yields the predicted net infiltration rates shown in Figure 6. The mean, median, maximum, and standard deviation of the differences between estimated and predicted net infiltration for the 94 intervals is −0.18, 0.12, 17, and 6.2 mm/yr, respectively, showing that there is no positive or negative bias in the average 21% misfit.

5.3. Net Infiltration Outside the Study Area

[28] For evaluating the accuracy of using the three surface parameters for predicting net infiltration rates to desert sandstone outside of the study area, vadose zone core samples were collected from a 35-m-deep borehole at Anderson Junction. Moisture cryodistilled from samples at 11 depths within the borehole yielded vadose zone ^{3}H concentrations ranging from 0.53 ± 0.03 to 8.4 ± 0.4 ^{3}H units (Figure 7). The maximum concentration, representing the 1963 peak in atmospheric ^{3}H from aboveground nuclear testing, was present at a depth of 12 m. On the basis of an average volumetric moisture content of 0.05 from land surface to this peak and a 40-year traveltime, a net infiltration rate of 15 ± 3 mm/yr was calculated by using the ^{3}H depth-to-peak method [*Cook et al.*, 1994]. This is about half of the empirically predicted net infiltration rate using equation (4) of about 30 mm/yr, based on the measured distance to the upgradient outcrop of more than 200 m, a soil having a particle size distribution 76% coarser than 0.15 mm, a measured topographic slope of about 5%, and

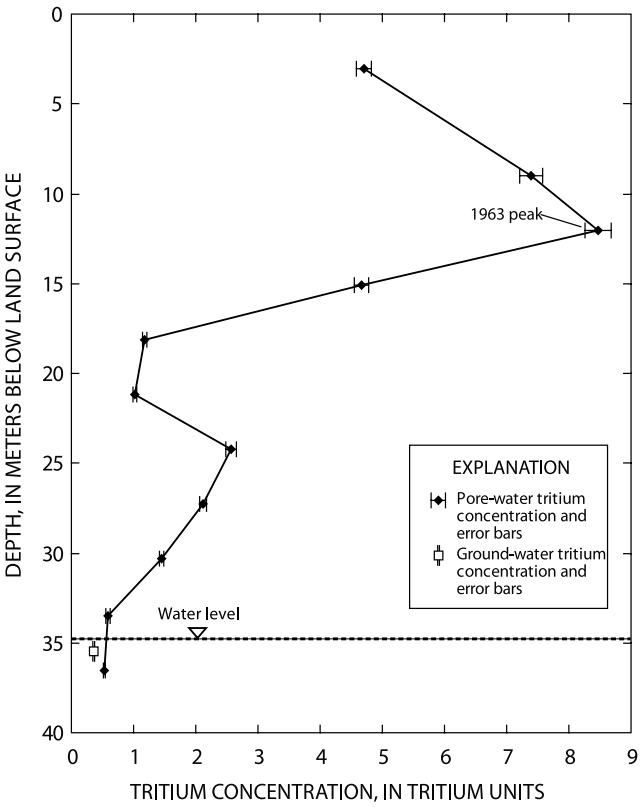

Figure 7. Vadose zone tritium profile of the borehole at Anderson Junction, Utah, October 2003.

an average annual modified PRISM precipitation rate of 276 mm. One likely factor for the lower actual versus predicted net infiltration rate is slope aspect. The Anderson Junction borehole site has a southeastern orientation (150°). It is assumed that less net infiltration occurs on slopes with southerly aspects because of higher evaporation rates associated with increased solar radiation.

5.4. GIS Modeling

[29] To estimate basin-scale net infiltration ratios, a GIS grid (10-m^2 cell size) representing the Sand Hollow study area was constructed with separate layers for soil coarseness, land surface elevation, and sandstone outcrop data. SSURGO soil maps [*Mortensen et al.*, 1977] and more recent field and areal photo mapping [*Sutcliffe*, 2005] provided the basis for the soil coarseness layer parameter, A_2. Particle size distributions of the SSURGO data did not coincide with the 0.15-mm sieve size, so laboratory analyses were run to determine a soil coarseness parameter for each of the 10 unique soil types present in the basin. These values (20% to 75%; Figure 8b) are similar to the range of coarseness values (18% to 80%) for soils adjacent to the trenches and road cut. A U.S. Geological Survey 10-m Digital Elevation Model (DEM) (National Center for Earth Resources Observation and Science (EROS), created in 1999, accessed April 2005 at http://ned.usgs.gov/) was used to calculate topographic slope for each cell. The resulting GIS layer for the topographic slope parameter, A_5, has values ranging from about 0% to 30% (Figure 8c), similar to 0.02% to 30% slopes along the excavations in Sand Hollow. Sandstone outcrop areas from the soils map and DEMs were combined for determining downgradient flow paths [*Tarboton*, 1997] for the distance-from-outcrop parameter, A_4. Downgradient influence was only calculated for flowpaths originating from outcrop areas (Figure 8d) and truncated to the 200-m maximum extinction distance.

[30] These three GIS data layers (soil coarseness, topographic slope, and downgradient distance from outcrop) provided the parameters used in equation (4) for determining net infiltration ratios for only the soil-covered parts of Sand Hollow. A constant net infiltration ratio of 0.10 was assigned to the remaining areas of outcropping sandstone and basalt boulder colluvium. For sandstone outcrop areas, this was based on both the ^{3}H-based ratio for borehole 43 of 0.13 (Table 2; the only site located on exposed sandstone) and previous Navajo sandstone infiltration studies at nearby Dirty Devil River [*Danielson and Hood*, 1984]. For the colluvium, this is based on an average estimated net infiltration ratio of 0.09 for intervals 62–68 and 73–94 (Table S1). Because of focused runoff from the basalt boulders, this ratio is larger than would be predicted on the basis of the soil coarseness of the sand/silt fraction of the colluvium. The colluvium, however, was not considered an outcrop area for the calculation of downgradient influence. These net infiltration ratios were then multiplied by the PRISM precipitation data (Figure 8a) to obtain predicted net infiltration rates.

[31] The GIS-based model predicts net infiltration rates ranging from 0 to 50 mm/yr for Sand Hollow (Figure 9), with a basin-scale average of 23 mm/yr. As predicted by the conceptual model (Figure 1), the areas with highest net infiltration rates (40–50 mm/yr) occur in coarser soils downgradient of sandstone outcrops. Medium net infiltration rates (20–40 mm/yr) occur in upland areas with coarser soils and higher precipitation rates, yet away from sandstone outcrops. The lowest net infiltration rates (0 to 20 mm/yr) occur beneath finer-grained soils not receiving runoff from sandstone outcrops. The herringbone patterns prominent in the bottom part of Figure 9 are the result of artifacts in the DEM.

5.5. Limitations

[32] The 21% average misfit between estimated and predicted net infiltration rates along the excavations (Figure 6) is likely caused by a 30-m sampling offset between sandstone excavations and soil sample locations. Because of the importance of soil coarseness in the empirical relation and its variability over small distances, the prediction of net infiltration rates is likely sensitive to such offsets. This is particularly important at or near mapped soil-type boundaries, such as those of the SSURGO soil maps [*Mortensen et al.*, 1977] and more recent field and areal photo mapping [*Sutcliffe*, 2005] within Sand Hollow. This may partly explain the relatively large differences between estimated and predicted net infiltration rates for intervals 7, 9, 34–35, 42–43, and 51–53. Large differences in some basalt boulder colluvium areas (intervals 64–67, 71, 73–74, 84–91) also contribute substantially to the overall misfit because (1) its soil coarseness varies more than other soil types, and (2) both focused infiltration of runoff from basalt boulders and the shadow effect on direct infiltration vary depending on boulder size and density.

[33] GIS-predicted net infiltration rates are generally similar to estimated rates at 11 borehole sites in Sand Hollow (Table 2). The GIS-predicted net infiltration rate at site 27 (20 mm/yr), however, is about five times higher than the ^{3}H-based net infiltration rate of 4 mm/yr. This site is located along an ephemeral wash at a boundary between a coarse (PTE) and a fine (Leb) soil. This exemplifies the fact that regional soils maps may not capture the detailed spatial heterogeneity associated with small features such as stream channel deposits and boundaries separating different soil types.

[34] The relatively large (100%) discrepancy between estimated and predicted net infiltration rates at the Anderson Junction borehole site outside of the study area shows that empirical methods developed with data from Sand Hollow need further investigation and refinement before they can be applied for quantifying absolute net infiltration rates in other desert sandstone locations. Other possible parameters controlling net infiltration that were not evaluated during this study include slope aspect, exposed outcrop parameters, and climate variables other than precipitation. Differences in slope aspect (and resulting differences in solar radiation) on net infiltration were not investigated because of the lack of southern exposures. Sand Hollow is predominantly north facing with aspects along the three excavations facing east, north, and west. Similarly, variations in other climate variables (including warm versus cold season precipitation, precipitation intensity/duration, temperature, relative humidity, and wind speed) likely affect net infiltration. The amount of precipitation and its timing also would control calcrete formation, affecting the permeability contrast at the soil/bedrock interface. Because net infiltration estimates for Sand Hollow are based on decadal to millennial accumulations of vadose zone environmental tracers, evaluating these precipitation variables was not possible. Finally, outcrop parameters such as area, fracture density, aspect, and slope

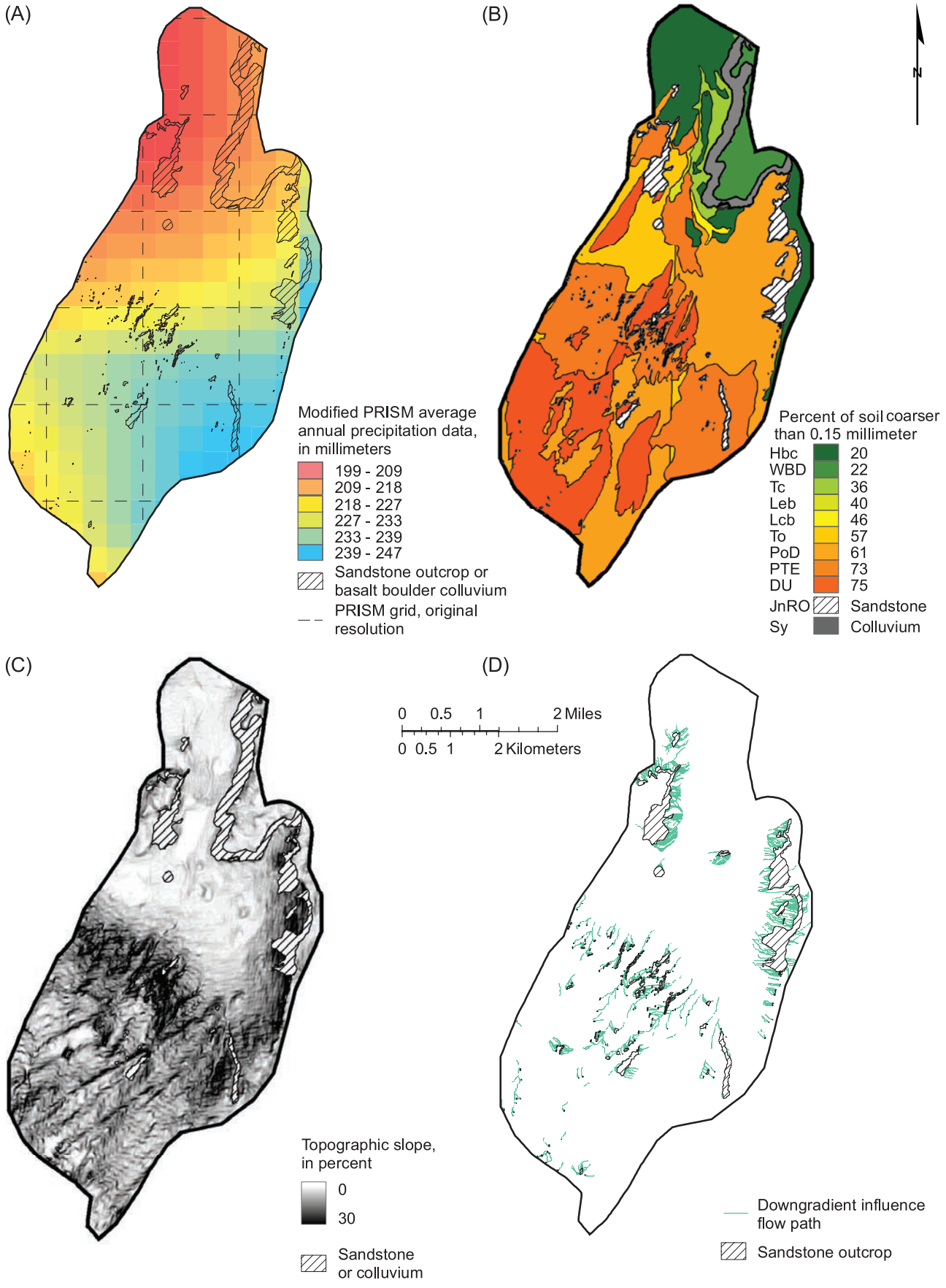

Figure 8. (a) Modified average annual PRISM precipitation, (b) soil coarseness, (c) topographic slope, and (d) downgradient influence flow paths from sandstone used to estimate net infiltration rates for Sand Hollow, Utah.

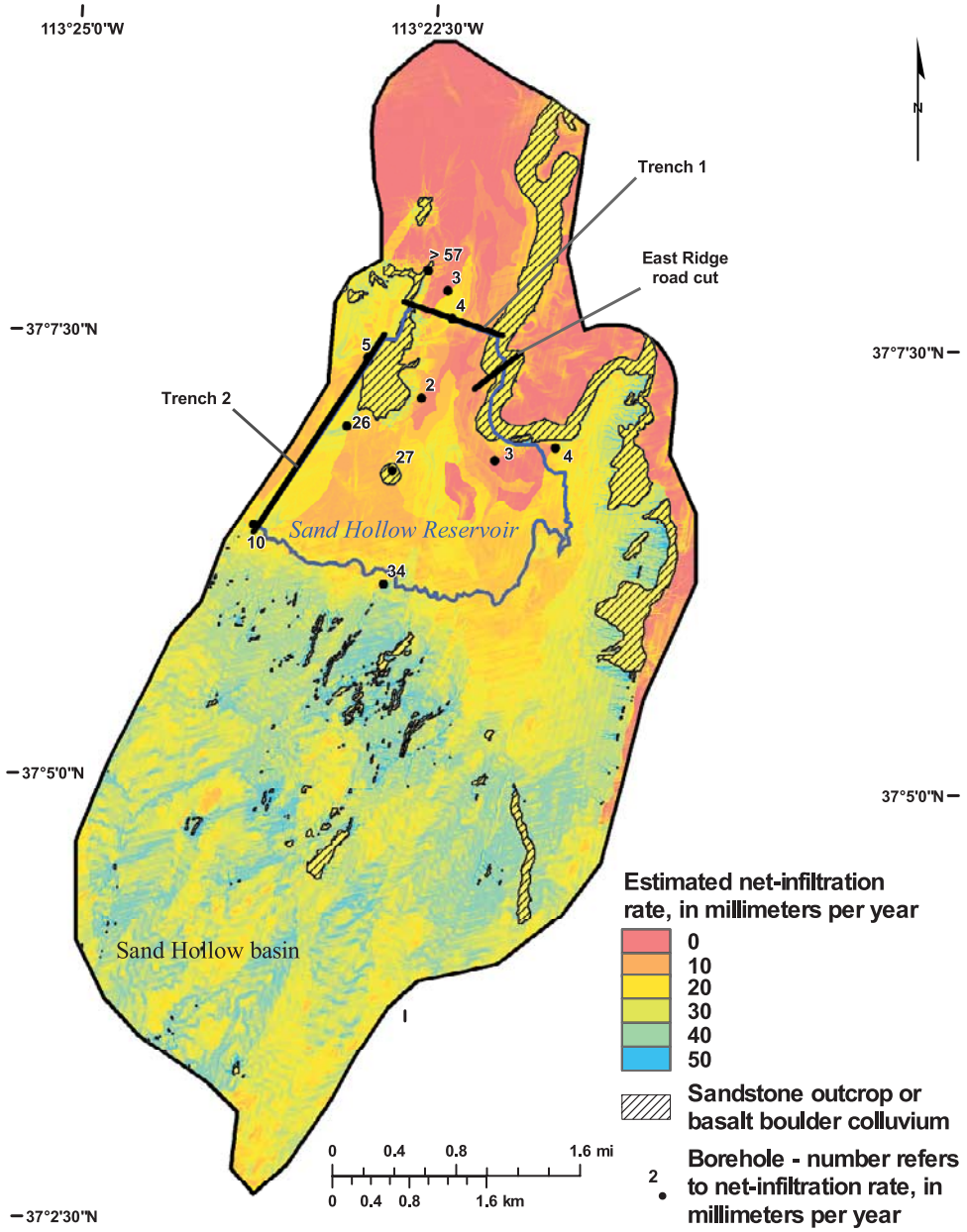

Figure 9. Predicted net infiltration rates for Sand Hollow, Utah.

would likely affect runoff volume, downgradient focused infiltration, and extinction distance. These were not evaluated during this investigation because only one large outcrop area was located upgradient of the excavations in Sand Hollow. As hypothesized above, larger, nonfractured, steeper, north facing outcrop areas would likely produce more runoff and therefore higher net infiltration rates in downgradient soil covered sandstone. Any combination of these factors may contribute to the discrepancy between estimated and predicted net infiltration rates at Anderson Junction.

6. Discussion

[35] The basin-scale average GIS-predicted net infiltration rate for Sand Hollow is 23 mm/yr, or about 10% of the basin-weighted average annual precipitation of 220 mm/yr. This is similar to recharge rates predicted by a previous numerical model covering a larger part of the Navajo aquifer of southwestern Utah [*Heilweil et al.*, 2000]. Although the spatial distribution of the GIS-predicted rates is based on vadose zone solutes (Cl, Sc), net infiltration values are determined by correlations between solute accumulation and borehole vadose zone ^{3}H using the depth-to-peak method rather than the Cl mass balance method. This approach was designed to take advantage of the much larger data set of solute concentrations along the 3350 m of excavations for describing the relative spatial variability in net infiltration, yet the more precise ^{3}H-based net infiltration rates at 11 borehole sites. The ^{3}H-based rates are considered more accurate because (1) as part of the water molecule, ^{3}H is considered a more conservative tracer of infiltration than Cl/Sc, (2) ^{3}H-based net infiltration rates in Sand Hollow have a smaller degree of uncertainty (±25%) than Cl-based

rates (±50%), primarily because of uncertainty in atmospheric Cl deposition rates, and (3) ^{3}H-based net infiltration rates at high-recharge borehole sites in Sand Hollow more closely correspond to groundwater Cl-based estimates than rates based on vadose zone Cl [*Heilweil et al.*, 2006]. In this previous work, recharge rates determined with the CMB method using water table Cl concentrations were compared to net infiltration rates determined from vadose zone borehole environmental tracers using (1) the CMB method with Cl from the soil/bedrock interface to the bottom of the Cl bulge, (2) the CMB method with Cl from the bottom of the bulge to the water table, (3) the ^{3}H depth-to-peak method. Four of these boreholes had high net infiltration rates and modern ^{3}H concentrations at the water table (1 to 7 TU), indicating recent recharge. Although net infiltration rates determined by using the three different vadose zone methods are well correlated, the ^{3}H-based rates (27 to >57 mm/yr) were most similar to the groundwater Cl-based rates (10 to 60 mm/yr), which best represent actual recharge rates. Vadose zone Cl rates from both within and below the Cl bulge had much lower values (2 to 8 mm/yr and 4 to 13 mm/yr, respectively). This comparison indicates a higher level of confidence in the ^{3}H-based rates, as compared with the vadose zone Cl-based rates, for determining absolute net infiltration rates. Precipitation records from 1893–2004 (Western Regional Climate Center, http://www.wrcc.dri.edu/), however, indicate that the latter half of the 20th century in southwestern Utah was slightly wetter than the 100-year average. The net infiltration rates calculated by using these GIS-predicted methods therefore reflect recent conditions (past 50 years) and may not be representative of conditions earlier in the Holocene.

[36] Because of its bedrock geology, the average basin infiltration rate of about 10% of precipitation for the Navajo sandstone at Sand Hollow is generally higher than that for alluvial study sites in the southwestern United States with similar arid climates. Recharge studies from alluvial sites suggest that little or no direct (interdrainage) recharge has been occurring during the late Holocene [*Phillips*, 1994; *Prudic*, 1994; *Tyler et al.*, 1996; *Andraski*, 1997; *Izbicki et al.*, 2002; *Scanlon et al.*, 2003; *Walvoord et al.*, 2002]. The net infiltration rates reported here are intermediate between low rates in these alluvial desert sites and higher rates reported in more humid settings [*Lorenz and Delin*, 2005; *Risser et al.*, 2005], but similar to net infiltration rates reported for fractured tuffs at Yucca Mountain, a similarly arid permeable bedrock setting [*Flint et al.*, 2001a]. This may be explained by the hydrologic characteristics of permeable bedrock, which permits moisture infiltration but not root penetration. The inability of roots to penetrate the nonfractured Navajo sandstone matrix and other consolidated permeable bedrock reduces the amount of plant evapotranspiration, thus increasing the percentage of infiltration available for net infiltration and recharge.

[37] Data analysis and interpretation at Sand Hollow indicate that three primary controlling parameters for net infiltration and recharge to desert sandstone are soil coarseness, distance from exposed outcrop, and topographic slope. In contrast, soil thickness and fracture density do not seem to play an important role. This is consistent with an earlier study showing a strong spatial correlation between soil coarseness (but not thickness) and locations where infiltration reached the underlying sandstone contact after an anomalously large precipitation event [*Heilweil and Solomon*, 2004]. A coarse soil will allow rapid gravity drainage to underlying bedrock regardless of thickness, whereas a fine soil will not. Regarding fracture density, the shallow parts of fractures beneath soil-covered areas generally are lined with low-permeability caliche; therefore they generally do not act as conduits for ponded water at the soil/sandstone interface. Furthermore, any moisture moving downward through unlined (open) sandstone fractures is quickly imbibed into the surrounding unsaturated sandstone. Thus it is assumed that low-permeability caliche and matrix imbibition are reasons why fracture density in soil covered areas is not a controlling factor in net infiltration and recharge.

[38] The concepts and methods developed for estimating net infiltration at Sand Hollow should be generally applicable for other areas of outcropping or soil-covered sandstone in arid climates and provide a reconnaissance-level assessment of its spatial variability. The accurate determination of absolute net infiltration rates in other settings, however, will likely require further investigation. Potential controlling parameters that were not within the scope of this study are (1) the physical characteristics (size, slope, aspect, and fracture density) of upgradient exposed outcrops, (2) topographic aspect of surficial soils, and (3) climatic parameters affecting evapotranspiration and calcrete formation. Investigation of the physical characteristics of exposed outcrops and their correlation to direct and focused infiltration was limited by both borehole and trench locations in Sand Hollow. Evaluating the topographic aspect of surficial soils on net infiltration also was limited by the lack of predominantly south facing aspects within Sand Hollow. The climatic parameters affecting the interplay between evapotranspiration, calcrete formation, and net infiltration (temperature, solar radiation, wind speed, and relative humidity) were assumed to be spatially constant within Sand Hollow. These parameters would vary in climates that are wetter and drier than that of Sand Hollow, but could not be analyzed within the scope of this study. Finally, the relation between precipitation and net infiltration may not be the same in areas receiving either more or less precipitation than Sand Hollow (200–250 mm/yr). Although a common assumption is that net infiltration ratios increase in wetter climates and decrease in drier climates, other regional factors likely play a role, such as warm versus cold season precipitation and average storm duration and intensity.

[39] An understanding of the spatial variability of net infiltration and recharge to desert sandstone at the basin scale is relevant to a number of scientific and societal needs. Two potentially important applications are (1) the accurate spatial distribution of recharge to regional groundwater flow models, and (2) land use zoning and groundwater source protection. In the case of Sand Hollow, a previously published [*Heilweil et al.*, 2000] groundwater flow model assigned a constant percentage of precipitation as direct (aerial) recharge to the water table. By comparing Figures 8a and 9, it can be observed that this would result in too much recharge to the southeastern and the northern parts of the basin, yet too little recharge in the southwestern area. With regards to land use zoning for source protection, net infiltration mapping can identify high net infiltration areas of a basin where the aquifer would be particularly susceptible to

surface contamination from sources such as septic effluent, road salt application, or chemical spills.

7. Summary

[40] Results of a linear inversion analysis combining estimated net infiltration rates along 3350 m of sandstone excavations with potential surficial controlling parameters resulted in the testing of a conceptual model and development of an empirical relation for predicting net infiltration to desert sandstone. Initial inversion modeling included potential controlling parameters requiring excavation, such as soil thickness and sandstone fracture density. Sensitivity analysis, however, showed that reducing this to only three surficial parameters (soil coarseness, distance from outcrop, and slope) did not decrease the accuracy of the empirical relation. This relation can be used with GIS data sets for basin-scale evaluation of net infiltration. This tool is useful for delineating recharge areas for both resource evaluation and source protection, but its accuracy is dependent upon the precision of the input data (soils map and outcrop delineations, topographic maps, soil coarseness analysis). The controlling parameters identified in this study for evaluating the spatial variability of net infiltration should be generally applicable for desert sandstone in other climatic settings. Accurate quantification of absolute net infiltration rates, however, will require independent evaluation of net infiltration using tools such as borehole environmental tracers.

Notation

A_1 soil thickness, m.
A_2 grain size, percent coarser than 0.15 mm.
A_3 sandstone vertical fracture density, number of fractures per linear meter.
A_4 downgradient distance from sandstone outcrop, m.
A_5 topographic slope, %.
Cl chloride concentration, mg/L.
$m_{1\text{-}15}$ model weighting functions.
R net infiltration ratio.
R_n N by 1 vector of observed data.
Sc leachate specific-conductance value, μS/cm.

[41] **Acknowledgments.** This project was supported by the Washington County Water Conservancy District, the U.S. Bureau of Reclamation, and the U.S. Geological Survey. The lead author benefited from detailed discussions with D. Kip Solomon of the University of Utah. Peter Cook, Geoffrey Delin, Mary Donato, and two anonymous reviewers provided very helpful peer review comments.

References

Allison, G. B., and M. W. Hughes (1974), Environmental tritium in the unsaturated zone: Estimation of recharge to an unconfined aquifer, in *Isotope Techniques in Groundwater Hydrology,* vol. 1, pp. 57–72, Int. At. Energy Agency, Vienna.

Allison, G. B., and M. W. Hughes (1978), The use of environmental chloride and tritium to estimate total recharge to an unconfined aquifer, *Aust. J. Soil Res.*, *16*, 181–195.

Allison, G. B., W. J. Stone, and M. W. Hughes (1985), Recharge in karst and dune elements of a semi-arid landscape as indicated by natural isotopes and chloride, *J. Hydrol.*, *76*, 1–25.

Allison, G. B., G. W. Gee, and S. W. Tyler (1994), Vadose-zone techniques for estimating groundwater recharge in arid and semiarid regions, *Soil Sci. Soc. Am. J.*, *58*, 6–14.

Anderson, L. J., and T. Sevel (1974), Six years' environmental tritium profiles in the unsaturated and saturated zones, Grønhøj, Denmark, in *Isotope Techniques in Groundwater Hydrology,* vol. 1, 3–20, Int. At. Energy Agency, Vienna.

Andraski, B. J. (1997), Soil-water movement under natural-site and waste-site conditions: A multiple-year field study in the Mojave Desert, Nevada, *Water Resour. Res.*, *33*, 1901–1916.

Ang, A. H.-S., and W. H. Tang (1975), *Probability Concepts in Engineering Planning and Design*, vol. 1, *Basic Principles*, John Wiley, New York.

Arnold, T., and M. Friedel (2000), Effects of land use on recharge potential of surficial and shallow bedrock aquifers in the Upper Illinois Basin, *U.S. Geol. Surv. Water Resour. Invest.*, 00–4027.

Braun, G. M., N. S. Levine, S. J. Roberts, and A. N. Samuel (2003), A geographic information systems methodology for the identification of groundwater recharge areas in Waukesha County, Wisconsin, *Environ. Eng. Geosci.*, *9*(3), 267–278.

Buttle, J. M., and D. J. McDonald (2002), Coupled vertical and lateral preferential flow on a forested slope, *Water Resour. Res.*, *38*(5), 1060, doi:10.1029/2001WR000773.

Cerling, T. E. (1984), The stable isotopic composition of modern soil and its relationship to climate, *Earth Planet. Sci. Lett.*, *71*, 229–240.

Charles, E., C. Behroozi, J. Schooley, and J. Hoffman (1993), A method for evaluating ground-water recharge areas in New Jersey, *N. J. Geol. Surv. Rep. GSR-32*, Trenton, N. J.

Cherkauer, D. S. (2004), Quantifying ground water recharge at multiple scales using PRMS and GIS, *Ground Water*, *42*(1), 97–110.

Cherkauer, D. S., and S. A. Ansari (2005), Estimating ground water recharge from topography, hydrogeology, and land cover, *Ground Water*, *43*(1), 102–112.

Clark, W. B., W. J. Jenkins, and Z. Top (1976), Determination of tritium by mass spectrometric measurements of ^{3}He, *Int. J. Appl. Radiat. Isot.*, *27*, 515–522.

Cook, P. G., G. R. Walker, and I. D. Jolly (1989), Spatial variability of groundwater recharge in a semiarid region, *J. Hydrol.*, *111*, 195–212.

Cook, P. G., W. M. Edmunds, and C. B. Gaye (1992), Estimating paleorecharge and paleoclimate from unsaturated zone profiles, *Water Resour. Res.*, *28*(10), 2721–2731.

Cook, P. G., I. D. Jolly, F. W. Leany, G. R. Walker, G. L. Allan, L. K. Fifield, and G. B. Allison (1994), Unsaturated zone tritium and chlorine 36 profiles from southern Australia: Their use as tracers of soil water movement, *Water Resour. Res.*, *30*(6), 1709–1719.

Cordova, R. M. (1978), Ground-water conditions in the Navajo sandstone in the central Virgin River basin, Utah, *Tech. Publ. 61*, Utah Dep. of Nat. Resour., Salt Lake City, Utah.

Cordova, R. M., G. W. Sandberg, and W. McConkie (1972), Ground-water conditions in the central Virgin River basin, Utah, *Tech. Publ. 40*, Utah Dep. of Nat. Resour., Salt Lake City, Utah.

Danielson, T. W., and J. W. Hood (1984), Infiltration to the Navajo sandstone in the lower Dirty Devil River basin, Utah, with emphasis on techniques used in its determination, *U.S. Geol. Surv. Water Resour. Invest.*, 84–4154.

Delin, G., R. Healy, M. Landon, and J. Bohlke (2000), Effects of topography and soil properties in recharge at two sites in an agricultural field, *J. Am. Water Resour. Assoc.*, *36*(6), 1401–1416.

Derby, N. E., and R. E. Knighton (2001), Field-scale preferential transport of water and chloride tracer by depression-focused recharge, *J. Environ. Qual.*, *30*, 194–199.

de Vries, J. J., and I. Simmers (2002), Groundwater recharge: An overview of processes and challenges, *Hydrogeol. J.*, *10*, 5–17.

Edmunds, W. M., E. Fellman, I. B. Goni, and C. Prudhomme (2002), Spatial and temporal distribution of groundwater recharge in northern Nigeria, *Hydrogeol. J.*, *10*, 205–215.

Eychaner, J. H. (1983), Geohydrology and effects of water use in the Black Mesa area, Navajo and Hopi Indian reservations, Arizona, *U.S. Geol. Surv. Water Supply*, 2201.

Flint, A. L., and L. E. Flint (2006), Modeling soil moisture processes and recharge under a melting snowpack, paper presented at TOUGH Symposium, Lawrence Berkeley Natl. Lab., Berkeley, Calif.

Flint, A. L., L. E. Flint, G. S. Bodvarsson, E. M. Kwicklis, and J. M. Fabryka-Martin (2001a), Evolution of the conceptual model of vadose zone hydrology for Yucca Mountain, *J. Hydrol.*, *247*, 1–30.

Flint, A. L., L. E. Flint, J. A. Havesi, and D. B. Hudson (2001b), Characterization of arid land infiltration processes at Yucca Mountain, Nevada, in *Flow and Transport Through Unsaturated Fractured Rock*, *Geophys. Monogr. Ser.*, vol. 42, edited by D. D. Evans, T. C. Rasmussen, and T. J. Nicholson, pp. 135–149, AGU, Washington, D. C.

Flint, A. L., L. E. Flint, E. M. Kwicklis, G. S. Bodvarsson, and J. M. Fabryka-Martin (2001c), Hydrology of Yucca Mountain, Nevada, *Rev. Geophys.*, *39*(4), 447–470.

Flint, A. L., L. E. Flint, E. M. Kwicklis, J. M. Fabryka-Martin, and G. S. Bodvarsson (2002), Estimating recharge at Yucca Mountain, Nevada, USA: Comparison of methods, *Hydrogeol. J.*, *10*, 180–204.

Flint, A. L., L. E. Flint, J. A. Hevesi, and J. M. Blainey (2004), Fundamental concepts of recharge in the Desert Southwest: A regional modeling perspective, in *Groundwater Recharge in a Desert Environment: The Southwestern United States*, *Water Sci. Appl. Ser.*, vol. 9, edited by J. F. Hogan, F. M. Phillips, and B. R. Scanlon, pp. 159–184, AGU, Washington, D. C.

Freeze, R. A., and J. A. Cherry (1979), *Groundwater*, pp. 604, Prentice-Hall, Englewood Cliffs, N. J.

Heilweil, V. M., and D. K. Solomon (2004), Millimeter- to kilometer-scale variations in vadose-zone bedrock solutes: Implications for estimating recharge in arid settings, in *Groundwater Recharge in a Desert Environment: The Southwestern United States*, *Water Sci. Appl. Ser.*, vol. 9, edited by J. F. Hogan, F. M. Phillips, and B. R. Scanlon, pp. 49–67, AGU, Washington, D. C.

Heilweil, V. M., G. W. Freethey, B. J. Stolp, C. D Wilkowske, and D. E. Wilberg (2000), Geohydrology and numerical simulation of groundwater flow in the Central Virgin River Basin of Iron and Washington counties, Utah, *Tech. Publ. 116*, Utah Dep. of Nat. Resour., Salt Lake City, Utah.

Heilweil, V. M., D. D. Susong, P. M. Gardner, and D. E. Watt (2005), Pre- and post-reservoir ground-water conditions and assessment of artificial recharge at Sand Hollow, Washington County, Utah, 1995–2005, *U.S. Geol. Surv. Sci. Invest.*, 2005–5185.

Heilweil, V. M., D. K. Solomon, and P. M. Gardner (2006), Borehole environmental tracers for evaluating net infiltration and recharge through desert bedrock, *Vadose Zone J.*, *5*, 98–120.

Holtschlag, D. J. (1997), A generalized estimate of ground-water recharge rates in the lower penninsula of Michigan, *U.S. Geol. Surv. Water Supply*, 2437.

Hood, J. W., and T. W. Danielson (1981), Bedrock aquifers in the lower Dirty Devil River basin area, Utah, with special emphasis on the Navajo sandstone, *Tech. Publ. 68*, Utah Dep. of Nat. Resour., Salt Lake City, Utah.

Hood, J. W., and D. J. Patterson (1984), Bedrock aquifers in the northern San Rafael Swell area, Utah, with special emphasis on the Navajo sandstone, *Tech. Publ. 78*, Utah Dep. of Nat. Resour., Salt Lake City, Utah.

Hurlow, H. A. (1998), The geology of the central Virgin River basin, southwestern Utah, and its relation to ground-water conditions, *Utah Geol. Surv. Water Resour. Bull.*, *26*, Utah Dep. of Nat. Resour., Salt Lake City, Utah.

Izbicki, J. A., R. L. Michel, and P. Martin (1998), Chloride and tritium concentrations in a thick unsaturated zone underlying an intermittent stream in the Mojave Desert, southern California, USA, in *Gambling with Groundwater—Physical, Chemical, and Biological Aspects of Aquifer-Stream Relations*, edited by J. V. Brahana et al., pp. 81–88, Ann Arbor Sci., Ann Arbor, Mich.

Izbicki, J. A., J. Radyk, and R. L. Michel (2002), Movement of water through the thick unsaturated zone underlying Oro Grande and Sheep Creek Washes in the western Mojave Desert, USA, *Hydrogeol. J.*, *10*, 409–427.

Klock, H. (2003), Hydrogeology of the Kalahari in north-eastern Namibia with special emphasis on groundwater recharge, flow modeling and hydrochemistry, *J. Hydrogeol. Environ.*, *31*, 1–194.

Kwicklis, E., M. Witkowski, K. Birdsell, B. Newman, and D. Walther (2005), Development of an infiltration map for the Los Alamos Area, New Mexico, *Vadose Zone J.*, *4*, 672–693.

Lorenz, D. L., and G. N. Delin (2005), Estimates of ground-water recharge in Minnesota, *Geol. Soc. Am. Abstr. Programs*, *37*(7), 32.

McCoy, J., K. Johnston, S. Kopp, B. Borup, and J. Willison (2001), *Using ArcGIS TM Spatial Analyst*, 232 pp., Environ. Syst. Res. Inst., Redlands, Calif.

Mortensen, V. L., J. A. Carley, G. C. Crandall, K. M. Donaldson, and G. W. Leishman (1977), *Soil Survey of Washington County, Utah*, 140 pp., U.S. Dep. of Agric., Soil Conserv. Serv., Washington, D. C.

Nitao, J. L., and T. A. Busheck (1991), Infiltration of a liquid front in an unsaturated fractured porous medium, *Water Resour. Res.*, *27*(8), 2099–2112.

Olofsson, B. (1994), Flow of groundwater from soil to crystalline rock, *Appl. Hydrogeol.*, *2*(3), 71–83.

Phillips, F. M. (1994), Environmental tracers for water movement in desert soils of the American Southwest, *Soil Sci. Soc. Am. J.*, *58*, 15–24.

Phillips, F. M., J. L. Mattick, and T. A. Duval (1988), Chlorine 36 and tritium from nuclear weapons fallout as tracers for long-term liquid movement in desert soils, *Water Resour. Res.*, *24*(11), 1877–1891.

Prudic, D. E. (1994), Estimates of percolation rates and ages of water in unsaturated sediments at two Mohave Desert sites, California-Nevada, *U.S. Geol. Surv. Water Resour. Invest.*, 94–4160.

Quade, J., T. E. Cerling, and J. R. Bowman (1989), Systematic variations in the carbon and oxygen isotopic composition of pedogenic carbonate along elevation transects in the southern Great Basin, United States, *Geol. Soc. Am. Bull.*, *101*, 464–475.

Rasmussen, T. C., and D. D. Evans (1993), Water infiltration into exposed fractured rock surfaces, *Soil Sci. Soc. Am. J.*, *57*, 324–329.

Risser, D. W., W. J. Gburek, and G. J. Folmar (2005), Comparison of methods for estimating ground-water recharge and base flow at a small watershed underlain by fractured bedrock in the eastern United States, *U.S. Geol. Surv Sci. Invest.*, 2005–5038.

Robson, S. G., and E. R. Banta (1995), Ground water atlas of the United States, segment 2: Arizona, Colorado, New Mexico, Utah, *U.S. Geol. Surv. Hydrol. Invest.*, *730-C*.

Scanlon, B. R. (1991), Evaluation of moisture flux from chloride data in desert soils, *J. Hydrol.*, *128*, 137–156.

Scanlon, B. R., R. W. Healy, and P. G. Cook (2002), Choosing appropriate techniques for quantifying groundwater recharge, *Hydrogeol. J.*, *10*, 18–39.

Scanlon, B. R., K. Keese, R. C. Reedy, J. Simunek, and B. J. Andraski (2003), Variations in flow and transport in thick desert vadose zones in response to paleoclimatic forcing (0–90 kyr): Field measurements, modeling, and uncertainties, *Water Resour. Res.*, *39*(7), 1179, doi:10.1029/2002WR001604.

Schlesinger, W. H. (1985), The formation of caliche in soils of the Mojave Desert, California, *Geochim. Cosmochim. Acta*, *49*, 57–99.

Sharma, M. L., and M. W. Hughes (1985), Groundwater recharge estimation using chloride, deuterium and oxygen-18 profiles in the deep coastal sands of western Australia, *J. Hydrol.*, *81*, 93–109.

Stephens, D. B. (1996), *Vadose Zone Hydrology*, 347 pp., CRC Press, Boca Raton, Fla.

Stothoff, S. A., D. Or, D. Groeneveld, and S. B. Jones (1999), The effect of vegetation on infiltration in shallow soils underlain by fissured bedrock, *J. Hydrol.*, *218*, 169–190.

Sukhija, B. S., and C. R. Shah (1976), Conformity of groundwater recharge rate by tritium method and mathematical modeling, *J. Hydrol.*, *30*, 167–178.

Sutcliffe, K. D. (2005), *Special Report of the Washington County, Utah Soil Survey*, U.S. Dep. of Agric., Soil Conserv. Serv., Washington, D. C.

Tarboton, D. G. (1997), A new method for the determination of flow directions and contributing areas in grid digital elevation models, *Water Resour. Res.*, *33*(2), 309–319.

Tindall, J. A., and J. R. Kunkel (1999), *Unsaturated Zone Hydrology*, 624 pp., Prentice-Hall, Upper Saddle River, N. J.

Tyler, S. W., J. B. Chapman, S. H. Conrad, D. P. Hammermeister, D. O. Blout, J. J. Miller, M. J. Sully, and J. M. Ginanni (1996), Soil-water flux in the southern Great Basin, United States: Temporal and spatial variations over the last 120,000 years, *Water Resour. Res.*, *32*(6), 1481–1500.

U.S. Bureau of Reclamation (1990a), Procedure for performing gradation analysis of gravel size fraction of soils, *USBR 5325-89*, in *Earth Manual*, *Part 2*, 3rd ed., pp. 323–330, Mater. Eng. Branch, Res. and Lab. Serv. Div., Denver, Colo.

U.S. Bureau of Reclamation (1990b), Procedure for performing gradation analysis of fines and sand size fraction of soils, including hydrometer analysis, *USBR 5330-89*, in *Earth Manual*, *Part 2*, 3rd ed., pp. 331–339, Mater. Eng. Branch, Res. and Lab. Serv. Div., Denver, Colo.

Vogel, J. C., L. Thilo, and M. Van Dijken (1974), Determination of groundwater recharge with tritium, *J. Hydrol.*, *23*, 131–140.

Walvoord, M. A., M. A. Plummer, F. M. Phillips, and A. V. Wolfsberg (2002), Deep arid system hydrodynamics: 1. Equilibrium states and response times in thick desert vadose zones, *Water Resour. Res.*, *38*(12), 1308, doi:10.1029/2001WR000824.

Wilson, J. L., and H. Guan (2004), Mountain-block hydrology and mountain-front recharge, in *Groundwater Recharge in a Desert Environment: The Southwestern United States*, *Water Sci. Appl. Ser.*, vol. 9, edited by J. F. Hogan, F. M. Phillips, and B. R. Scanlon, pp. 113–138, AGU, Washington, D. C.

Zhdanov, M. S. (2002), *Geophysical Inverse Theory and Regularization Problems*, 609 pp., Elsevier, Amsterdam.

V. M. Heilweil and T. S. McKinney, U.S. Geological Survey, Salt Lake City, UT 84119, USA. (heilweil@usgs.gov)

D. E. Watt, U.S. Bureau of Reclamation, Boulder City, NV 89005-1470, USA.

M. S. Zhdanov, Department of Geology and Geophysics, University of Utah, Salt Lake City, UT 84112-0111, USA.